Interaction between Medetomidine and Alkyd Resins: NMR and FTIR Investigation of Antifouling Marine Paint Model Systems

Liubov Shtykova,[1] Denis Ostrovskii,[2] Per Jacobsson,[2] Magnus Nydén[1]

[1]*Department of Materials and Surface Chemistry, Chalmers University of Technology, SE-412 96, Göteborg, Sweden*
[2]*Department of Applied Physics, Chalmers University of Technology, SE-412 96, Göteborg, Sweden*

Received 29 December 2004; accepted 8 April 2005
DOI 10.1002/app.22847
Published online 19 December 2005 in Wiley InterScience (www.interscience.wiley.com).

ABSTRACT: The synthesis and optimization of novel bioactive components is key to the development of antifouling marine coatings. It was recently demonstrated that medetomidine (MM) has perfect antibarnacle behavior along with good ecological properties. To investigate the applicability of MM in self-polishing marine paints, a large set of mixtures of MM with two commercial alkyd resins (ARs) was prepared. The nature and strength of the intermolecular interaction as a function of composition in both the liquid and solid states were studied using NMR and FTIR techniques, respectively. It was found that at low concentrations MM molecules were coordinated to alkyd resin chains by hydrogen bonding. This interaction had a multidentate character (i.e., one molecule of MM interacted with several —COOH species of ARs) that resulted in stronger bonding between the two compounds. However, at higher MM concentrations an ionic association between the two compounds began, which at a large MM content resulted in microphase separation. It was noted that the strong interaction between medetomidine and the alkyd resins investigated was a positive factor for the application of these compounds in self-polishing marine paints. © 2005 Wiley Periodicals, Inc. J Appl Polym Sci 99: 2797–2809, 2006

Key words: NMR; FTIR; coatings

INTRODUCTION

The main problem with materials immersed in seawater is fouling (or biofouling), that is, the settlement and growth of a variety of biological species and/or organisms on the surface of a material. Although fouling poses no essential problems for static objects (pipes, cables, navigation buoys, etc.), it may cause serious problems for ship hulls, for example. For instance, increased surface roughness from fouling may result in a 40% increase in a vessel's fuel consumption, not counting the additional cost of cleaning and repainting.[1,2] Attempts to overcome fouling have occurred for more than 4,000 years—in 2000 BC ships were fastened with copper bolts and their bottoms were covered with lead.[3] Since the 19th century paints containing a special ingredient to prevent settlement of microorganisms, a so-called antifoulant (AF) or antifouling agent, have been produced industrially.[3] Antifoulants must, on the one hand, effectively prevent the growth of various marine organisms, the variety of which runs to more than 1700 species,[4] and, on the other hand, should not be hazardous to marine ecology in general. Thus, creating a proper antifouling agent is key to the development of novel marine paints. So far, hundreds of materials have been thoroughly tested for use as AFs. Omae[5,6] recently reviewed the latest achievements in this field.

For many decades, biofouling was mostly controlled with the use of a large variety of metal biocides such as copper and organotin compounds. However, it was found that despite having a high degree of efficiency, these materials had a very negative effect on nontarget species. Therefore, their application is now strongly regulated and even banned around the world. Thus, in the last 15–20 years less toxic and more environmentally friendly antifoulants have been intensively developed. To shorten the time and cost of development, it has been proposed[7,8] that pharmaceuticals be used as antifoulants. These compounds have known chemistries and mechanisms from investigations in human and animal models. Medetomidine ($C_{13}H_{16}N_2$), or ^{1}H-imidazole, 4-[1-(2,3-dimethylphenyl)ethyl], is a well-known bioactive compound and is widely used in medicine.[9–11] Its chemical structure is shown in Figure 1(a). In recent testing of its potential use as an antifouling agent in marine paints,[12,13] this molecule was found to be very microbiologically active against the fouling of various barnacles, which are

Correspondence to: L. Shtykova (lyuba@chem.chalmers.se).
Contract grant sponsor: MISTRA (Swedish Foundation for Environmental Research).

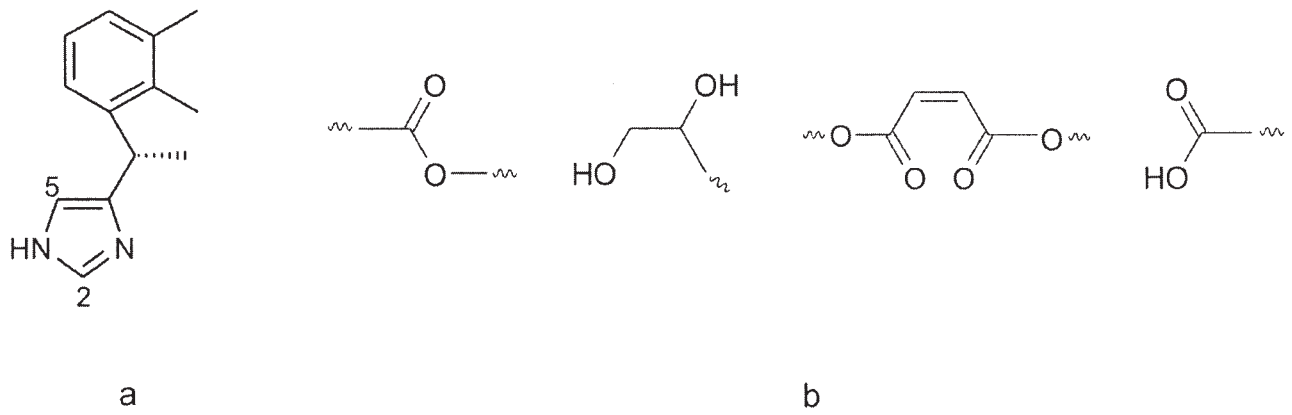

Figure 1 Chemical structure of (a) medetomidine and (b) main fragments of alkyd resin (numbers 2 and 5 indicate the positions of specific protons, discussed in the text).

hard fouling organisms, making medetomidine a candidate for use in industrial marine paints.

Another significant aspect of paint formulation is the compatibility of the components used. A typical marine paint is a complex mixture of about 10 compounds,[14] both organic and inorganic. The likely most important factor in bioactivity is the interaction between the AF and the polymer binder, which is the dominant organic component of a paint film. The strength of this interaction controls the rate of antifoulant release. If the interaction is weak or absent, the AF will easily escape the system, thereby reducing the lifetime of the antifouling efficiency. In contrast, a very strong interaction in essence will restrict the biological effect. Thus, the creation and development of new advanced AFs immediately necessitates investigation of their interaction with the polymer materials already used in paint systems. In previous studies[12,13,15] the interaction between medetomidine and several polymers was investigated. In particular, it was found[12] that medetomidine showed a strong affinity for polystyrene and displayed a tendency to accumulate on both hydrophobic and hydrophilic polystyrene surfaces.[13] In a recent work[15] we investigated the interaction between medetomidine and long-oil alkyd resin, which is a typical polymer binder in industrial paints.[16] It appeared that AF molecules mostly bonded to the binder via hydrogen bonding and/or ionic pairing between carboxylic groups of the polymer and NH species of medetomidine. Such bonding provided reasonably good AF retention–release properties. In addition, these systems showed good integrity, and no phase separation was detected, even at high AF concentrations. However, it could be different with other polymers. Therefore, further investigation was needed in order to clarify the applicability of medetomidine in the wide spectrum of marine paints.

In the present work we applied NMR diffusometry and FTIR spectroscopy to the investigation of the interaction of medetomidine with two types of alkyd resins used as polymer binder in self-polishing marine paints. A large set of model systems with varying polymer–AF ratios was thoroughly investigated with the primary goal of clarifying the strength and the mechanisms of intermolecular interactions. Polymer–antifoulant coordination was studied in liquid solution by NMR diffusometry and in solid solvent-free films by FTIR.

EXPERIMENTAL

Chemicals and sample preparation

Fully deuterated *o*-xylene (*o*-xylene-d_{10}) was purchased from Dr. Glaser AG (Basel, Switzerland); the alkyd resins Syratal 11.5 (ST-11) and Syratal 23 (ST-23)—the number indicates the acid number—were kindly donated by Eastman Chemical Sweden AB (Mölndal, Sweden) and were used without further purification. The weight percent of fatty acids was approximately 60 wt % in both alkyd resins. The theoretical molecular weights of ST-11 and ST-23 were 1600 and 1200 g/mol, respectively. The medetomidine {(*S,R*)-4(5)-[1-(2,3-dimethylphenyl)ethyl] imidazole} was synthesized in accordance with a procedure previously described by Shtykova et al.[15] The chemical structures of medetomidine (MM) and of selected fragments of the alkyd resins (ARs) are presented in Figure 1.

The solutions were prepared as follows. First, enough medetomidine was dissolved in *o*-xylene-d_{10} to make 0.4 wt % (maximum solubility). Then, different amounts of polymer were added to the solution such that the polymer-to-medetomidine ratio, C_p/C_m, varied from 1 to 60. C_m and C_p are the concentrations by weight percent of MM and AR, respectively. A higher value of the C_p/C_m parameter corresponds to an increase in the relative content of alkyd resin at fixed concentrations of medetomidine.

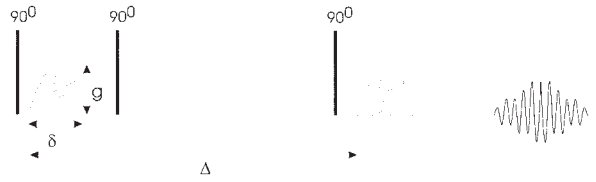

Figure 2 Pulsed gradient stimulated spin-echo (PGSSE) pulse sequence with sine-shaped gradient, where δ is the length, g is the strength of the gradient pulse, and Δ is diffusion time.

NMR experiments

^{1}H-NMR and NMR diffusometry experiments were conducted on Varian Unity Inova 600- and 500-MHz spectrometers, respectively, at 20°C. Diffusometry measurements were performed using a stimulated echo sequence, presented in Figure 2, with 40 gradients of varying strength (g) ranging from 0.02 to 1.6 Tm^{-1}, a gradient duration (δ) of 0.004 s, and diffusion time (Δ) of 0.07 s. The combinations of g, δ, and Δ were chosen in order to obtain 90–95% total signal attenuation at the highest g value. A sine-shaped gradient pulse was used to minimize the effect of eddy currents. All experiments were performed in 5-mm NMR tubes. The tubes were flame-sealed after vacuum removal of dissolved oxygen.

Calculation of self-diffusion coefficients

Analysis of the diffusion NMR data was performed with specialized software called CORE (component resolved spectroscopy).[17,18] CORE evaluates the diffusion data by a global least-squares fit. By this method, spectra of the individual components are calculated by a complete band-shape analysis, along with the corresponding diffusion coefficients. In a NMR diffusometry experiment using line-shaped gradients, the signal intensities of monodisperse molecules such as medetomidine and *o*-xylene obey a simple relationship:

$$I = I_0\exp(-kD),$$

where I_0 is signal intensity at $g = 0$, D is the diffusion coefficient, and k is $\delta^2 g^2 \gamma^2 (4\Delta - \delta)/\pi^2$ where γ is the gyromagnetic ratio.

For polydisperse systems such as alkyd resins with little or no signal overlap, signal intensity was evaluated by a standard least-squares fit method in MATLAB according to

$$I = I_0\int_0^\infty P(D)\exp(-kD)dD.$$

For many polydisperse mixtures the distribution function, $P(D)$, is well represented by a log-normal distribution

$$P(D) = \frac{1}{D\sigma_{\ln D}\sqrt{2\pi}}\cdot\exp\left[-\frac{(\ln D - \ln D_m)^2}{2\sigma_{\ln D}^2}\right],$$

where D_m is the median self-diffusion coefficient and $\sigma_{\ln D}$ is the standard deviation of the logarithm of the diffusion coefficient.

In more complex system, such as medetomidine–alkyd resin–xylene, in which NMR signals overlap, the log-normal distribution is the diffusion coefficient plus two single diffusion coefficients that describe the data well:

$$I/I_0 = f_1\int_0^\infty P(D_1)\exp(-kD_1)dD + f_2\exp(-kD_2) + (1 - f_1 - f_2)\exp(-kD_3)$$

where $f_{1,2,3}$ are the normalized fractions and $D_{1,2,3}$ are the diffusion coefficients of the three components. However, because of strong overlap of NMR signals, there were difficulties in using this function directly to evaluate the individual diffusion coefficients in the three-component mixture. So the diffusion coefficient of alkyd resins was evaluated from nonoverlapped NMR signals and than used as a fixed value in the last equation.

FTIR–ATR measurements

FTIR spectra were recorded at room temperature using a Bruker-IFS 66v spectrometer equipped with a liquid nitrogen–cooled MCT detector and attenuated total reflection (ATR) utility (45° ZnSe prism, a product of Graseby Specac). To record the spectrum, a certain amount of medetomidine-resin solution in *o*-xylene-d_{10} was sprayed on the surface of the horizontal ATR prism placed in the vaccumated sample compartment of the spectrometer. The solvent was allowed to evaporate for 5 min under vacuum (5 mbar) such that a solid film was formed. After that, the infrared spectrum was recorded. Every spectrum presented in this work represents the accumulation of 200 scans at a spectral resolution of 2 cm^{-1}.

RESULTS AND DISCUSSION

^{1}H-NMR spectra

Figure 3 presents ^{1}H-NMR spectra of pure ST-11 and ST-23 alkyd resins and their mixtures with medetomidine at $C_p/C_m = 4$. The solvent, *o*-xylene-d_{10}, showed two strong peaks at 2.0 (s, 6H) and 7.0 (d, 4H) ppm

(marked peaks). The medetomidine signal appeared at 1.6 (d, 3H), 2.2 (s, 3H), 2.3 (s, 3H), 4.4 (q, 1H), 6.6 (s, 1H), 6.9–7.0 (m, 3H) and 7.14 (s, 1H) ppm. The analysis of the spectrum of AR was too complicated to be assigned in detail, but the main peaks were noted as being in regions 0.8–3.1, 3.5–5.7, 6.4–8.0 ppm. The NMR spectra of ST-11 and ST-23 alkyd resins were very similar [Fig. 3(a,c)]. In both materials the high-field region of the proton spectra, 0.8–3.2 ppm, contained mainly methylene and methyl peaks from fatty acid protons. The 3.5–6.0 ppm region was characteristic of the protons neighboring ester and hydroxyl groups, and the 6.0–8.0 ppm envelope contained the signatures of aromatic protons of phthalic ester fragments.

The most noticeable difference between the spectra of the ST-11 and ST-23 polymers was observed in regions 0.8–2.5, 3.5–4.0, and 6.8–7.5 ppm. The number of peaks and their positions were the same for both materials, but the intensity of the signals differed. To study structural differences, we integrated the signals in these regions, and apparently in all three regions the integral intensity of the NMR signal was higher in the ST-23 resin spectrum. This observation shows that the amount of phthalic ester and acid fragments, as well as of methyl and methylene groups, was higher in ST-23. The signal at 6.2 ppm was chosen as the normalization intensity.

In the spectra of the medetomidine/polymer mixtures [Fig. 3(b,d)], we noted a strong overlap of the characteristic proton resonance peaks of the two components. This occurred because many different signals came from the polymer, and these were broadened

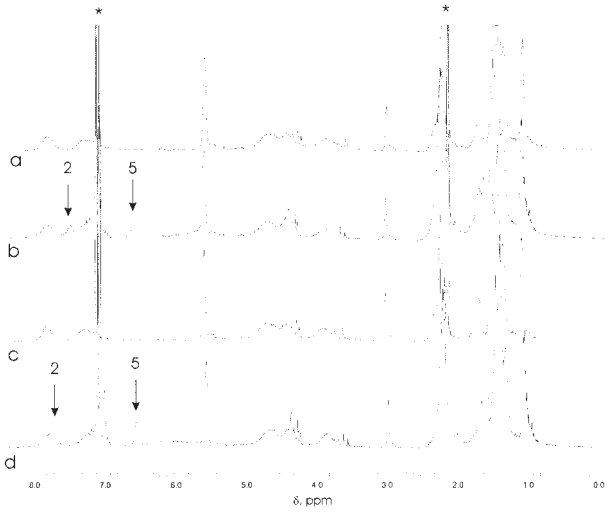

Figure 3 ^{1}H-NMR spectra of different solutions in *o*-xylene: (a) ST-11 (6 wt %), (b) mixture of ST-11 and MM (C_p/C_m = 3.75), (c) ST-23 (6 wt %), (d) mixture of ST-23 and MM (C_p/C_m = 3.75). The numbers 5 and 2 indicate the peaks of specific MM protons [see Fig. 1(a)]; asterisks indicate solvent peaks.

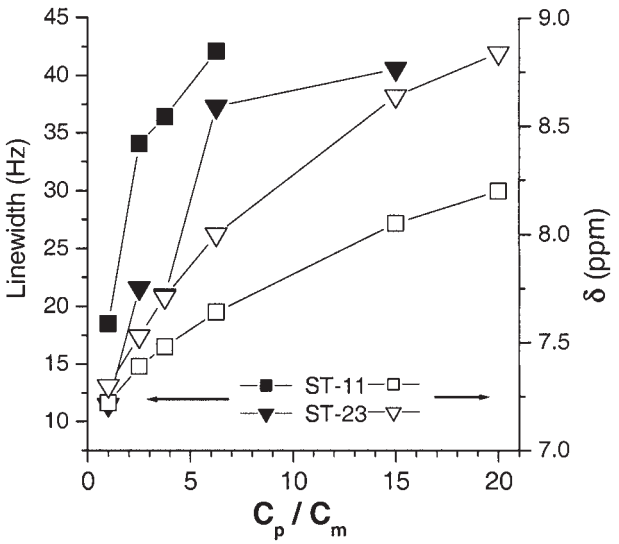

Figure 4 Variation of some NMR band parameters in AR–MM mixtures as a function of composition (solid symbols: line width of the MM proton 5; open symbols: chemical shift of MM proton 2).

because of the relatively short T_2 relaxation time. Nonetheless, a few characteristic peaks of individual components could still be resolved. A shift of the NMR signal and broadening of a specific region in the medetomidine/polymer spectrum were observed. The signals at 6.6 and 7.15 ppm referred to medetomidine protons 1 and 2, respectively (Fig. 1). It can be seen in the marked area of Figure 2 that the medetomidine peak at around 6.6 ppm broadened with increasing polymer concentration. In addition, the medetomidine peak originally at 7.14 ppm shifted to higher parts per million values as the polymer concentration increased. This behavior was observed for both ST-11 and ST-23. The changes are summarized in Figure 4, which shows the dependence of line width and position of the characteristic NMR signals of medetomidine for the different C_p/C_m ratios. It can be clearly seen for both polymers that when the C_p/C_m ratio increased, the NMR signal originally at 7.14 ppm shifted to higher values and that the signal at 6.6 ppm broadened with increasing polymer concentration. The change in line width most likely occurred because of an interaction between medetomidine and the alkyd resins. According to the results, changes in both the position and width of the medetomidine signals were stronger for ST-23 than for ST-11. We suggest that the interaction between medetomidine and the polymer with the higher acid number (ST-23) was stronger than that between medetomidine and the polymer with the lower acid number (ST-11). The medetomidine–solvent interactions could be neglected because of the aprotic apolar nature of *o*-xylene.[19]

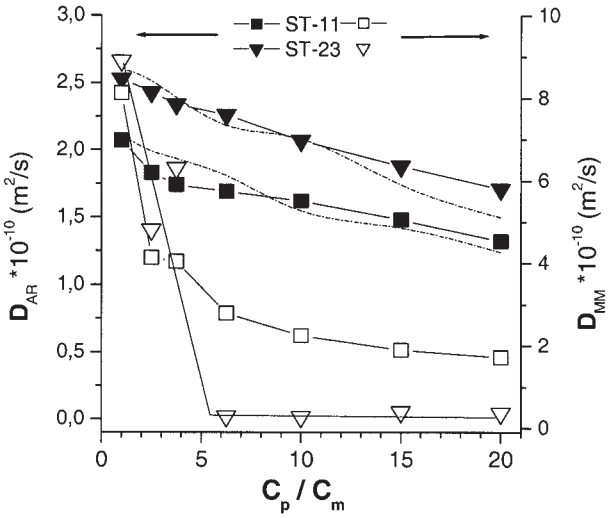

Figure 5 Dependence of self-diffusion coefficients of medetomidine and alkyd resins on mixture composition, evaluated by CORE (a dashed line indicates the self-diffusion coefficient of pure alkyds at the corresponding concentration).

NMR diffusometry

To estimate the strength of the interaction in the medetomidine–alkyd resin mixtures, the diffusion coefficients of MM, AR, and *o*-xylene were studied by NMR diffusometry for different mixture compositions. The dependence of the self-diffusion coefficient for AR is presented in Figure 5 (solid symbols). It can clearly be seen that the diffusion coefficients of both resins decreased linearly with increasing C_p/C_m. Similar behavior was found for pure AR at increasing concentration (dashed lines in Fig. 5). Hence, the addition of medetomidine did not influence the diffusion behavior of the alkyd resins. The observed behavior can be easily explained by a polymer concentration effect: a higher polymer content resulted in slower diffusion because of increased obstruction. Moreover, the diffusion coefficient dependence on concentration was the same in both cases. This reflects that the diffusion mechanism was the same for the two polymer systems. However, the values of the diffusion coefficients of the two polymers differed, with the self-diffusion of ST-11 polymer slower than that of ST-23 at all concentrations. This was most likely because of the higher molecular weight of the ST-11 polymer.

A similar diffusion behavior was observed for *o*-xylene at varying C_p/C_m ratios. Xylene diffused 1.4 times slower than pure xylene at $C_p/C_m = 20$. The diffusion behavior of xylene at an increasing C_p/C_m ratio can also be explained by obstruction of the solvent by the polymer.

In contrast, the dependence of the medetomidine self-diffusion coefficient (D_{MM}) on the C_p/C_m ratio was nonlinear (open symbols in Fig. 5) in the presence of AR. Two zones were clearly observed: a sharp decrease of D_{MM} until $C_p/C_m \sim 7$, followed by constant value of D_{MM} in the $C_p/C_m = 7$–20 region. A sharp reduction in D_{MM} at low C_p/C_m ratios suggests a restriction in the diffusional motion of MM by an interaction with the much larger polymer molecule. When fast exchange occurred, the measured average diffusion coefficient of MM included the diffusion of free and polymer-bound medetomidine molecules:

$$D_{MM} = x_f D_f + x_b D_b, \quad (1)$$

where D_f and D_b are the diffusion coefficients of the free and bound MM molecules, respectively; and x_f and x_b are their normalized fractions, respectively. The variation in polymer content, that is, in the C_p/C_m ratio, affected the fraction of free medetomidine, which was reflected by the D_{MM} values. At low C_p/C_m ratios, the free medetomidine dominated, but at higher C_p/C_m ratios, the fraction of x_b became larger. The fraction of bound MM molecules at increasing C_p/C_m was calculated and is presented in Table I. This value neared 1 at C_p/C_m ratios increasing from 1 to 20 for both the ST-11 and ST-23 alkyd resins. The x_b threshold value shown in Table I suggests there was saturation of the AR active groups with which medetomidine could interact. The saturation threshold started at a lower MM concentration for ST-23 than for ST-11, indicating that the strength of the intermolecular interaction between MM and the alkyd resins was stronger for ST-23 than for ST-11.

The number of binding sites for MM on AR reflects the binding capacity of AR to the MM molecule. Carboxylic groups in the polymer and an amino group in the MM were assumed to be active sites. The molar ratios between these two active sites, α = mol —NH/mol —COOH, were estimated and are presented in Table I. A comparison of the α values (Table I) with MM diffusion (see Fig. 5) can determine a threshold α value. These α values were 1 : 0.26 and 1 : 0.51 for

TABLE I
Fraction of Bound Medetomidine Molecules in AR-MM Mixtures (x_b) and Molar Ratio of $NH_{(MM)}$ and $COOH_{(AR)}$ groups (α) as a function of C_p/C_m Value

	x_b		α	
C_p/C_m	ST-11	ST-23	ST-11	ST-23
1	0.1	0.14	25 (0.04 : 1)	11 (0.09 : 1)
2.5	0.66	—	9.0 (0.11 : 1)	4.8 (0.21 : 1)
4	0.67	0.37	6.3 (0.16 : 1)	3.2 (0.31 : 1)
6.25	0.84	0.69	3.8 (0.26 : 1)	1.9 (0.51 : 1)
10	0.90	1.0	2.4 (0.41 : 1)	1.2 (0.81 : 1)
15	0.90	1.0	1.7 (0.6 : 1)	0.8 (1.2 : 1)
20	0.90	1.0	1.3 (0.8 : 1)	0.6 (1.7 : 1)
40	—	—	0.63 (1.6 : 1)	0.31 (3.2 : 1)
60	—	—	0.42 (2.4 : 1)	0.21 (4.7 : 1)

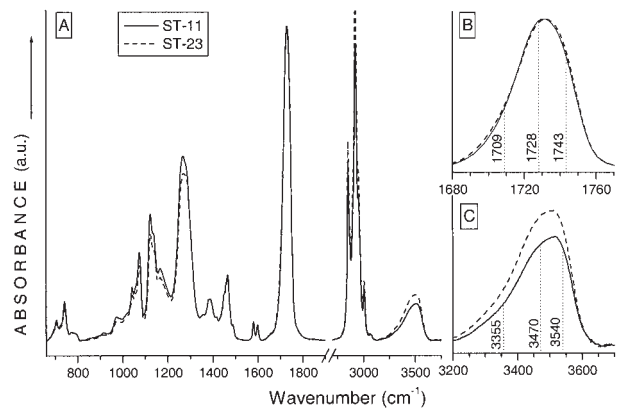

Figure 6 Comparison of FTIR spectra of two alkyd resins. The spectra were normalized using the intensity of CO stretching vibrations around 1730 cm^{-1}.

ST-11 and ST-23, respectively. Therefore, the binding capacity of the ST-23 alkyd resin to MM was higher than that of ST-11.

FTIR spectroscopy

Alkyd resins

The FTIR spectra of the two alkyd resins, shown in Figure 6(a), were found to be very similar to each other. Only small intensity redistribution between some spectral bands was noted. Thus, for instance, the ratio of relative intensities in the spectral intervals 1000–1300 cm^{-1} (various C—C modes) and 2750–3100 cm^{-1} (CH_2 and CH_3 stretching vibrations) differed, which definitely was a result of the differences in chain length in the two types of ARs. However, we were most interested in the behavior of carbonyl (—C═O) and hydroxyl (—OH) groups because these were the species that likely were responsible for the intra- and intermolecular interactions in the system.

In the FTIR spectrum of neat alkyd resins the characteristic band of C═O stretching vibrations appeared as a strong, broad, and asymmetric peak centered at about 1730 cm^{-1} [Fig. 6(a,b)]. Comprehensive curve fitting analysis of this envelope showed at least three components, at 1709, 1728, and 1743 cm^{-1}, respectively. Such a multicomponent structure can be easily understood because alkyd resins basically contain three types of carbonyl groups [see Fig. 1(b)]: carboxylic (—COOH), ester (—CH_2—CO—O—), and maleic (—O—CO—CH═CH—CO—O—). Taking into account that the frequency of C═O stretches is dependent on the group environment, it is reasonable to suggest that the presence of three distinct but quite similar species was responsible for the formation of the observed band shape. In agreement with data reported in the literature,[20] characteristic frequencies of carboxylic C═O groups fell into the region of 1700–1725 cm^{-1}, whereas carbonyl groups in ester/maleic configurations generated a band in the 1725–1750 cm^{-1} spectral envelope. Therefore, given the spectrum of alkyd resin, we tentatively assigned the low-frequency component of the CO stretching band (~1710 cm^{-1}) to the carboxylic C═O groups, and the components with higher frequencies (~1730 and ~1740 cm^{-1}) to the species in ester and maleic environments. We also noted that the relative intensities of the components at 1728 and 1743 cm^{-1} were slightly different in both materials [Fig. 6(b)]. This may have been a result of either a different number of corresponding C═O species or of differences in the intra- and interchain coordination in the two matrices. The latter, in turn, may have arisen because of significant differences in the molecular weight and specific content of free carboxyl groups in both types of ARs.

The characteristic spectral profile of the OH stretching vibrations in investigated alkyd resins [Fig. 6(c)] consists of three well-resolved bands centered at ~3355, ~3470, and ~3540 cm^{-1}, respectively. On the basis of data reported in the literature,[20] the high-frequency mode can be attributed to the carboxylic OH groups (—COOH), whereas the mode at 3470 cm^{-1} originated from the OH species in a —CH_nOH environment (alcohol type). The origin of the third component (~3355 cm^{-1}) is not straightforward. Taking into account the structural peculiarities of the materials [Fig. 1(b)], the presence of OH species in an environment different from the two discussed above is hardly possible. On the other hand, the frequency of OH vibrations is known to be sensitive to the strength of hydrogen bonding and shows a downward shift as this strength increases.[21] Therefore, we tentatively assigned the component with the lowest frequency to the strongly bonded hydroxyl groups.

Also interesting is that, as mentioned above, the spectra shown in Figure 6 were normalized with the intensity of C═O band. On the other hand, under such normalization total intensity of ν(OH) band appeared to be visibly higher in ST-23 [Fig. 6(c)]. This automatically signaled a higher content of polyhydric alcohol segments in this material. Thus, it became obvious that ST-23 contained not only a larger amount of free carboxyl groups (as determined from the acidic number) but also more polyol chains. Therefore, it was reasonably expected that the ST-23 binder would be more active in intermolecular interactions and hydrogen bond formation.

Medetomidine

Analyzing the spectral bands of medetomidine apparently was quite complicated for two reasons: (1) in the samples of special interest, whose AR–MM ratio was close to industry standards, the amount of MM was usually much lower than that of alkyd resin, and (2)

most of the MM bands strongly overlapped with those of AR. Therefore, it is nearly impossible to carefully consider the spectral behavior of most bands. However, it was possible to perform a detailed analysis of the peaks falling into the spectral interval of 750–870 cm^{-1}, which was practically free of any alkyd contribution (see Fig. 7). In this envelope the infrared spectrum of medetomidine contained two intense complexly structured absorption bands at 782 and 825 cm^{-1}. To clarify the origin of these features, we prepared a deuterated analog of medetomidine. In fact, the pyrrole nitrogen of the imidazole ring was readily deuterated by dissolution in D_2O because of a rapid exchange with solvent protons.[22] Thus, in the *N*-deuterated compound the vibrational modes related to the imidazole part of the molecule were expected to show a frequency shift and/or intensity changes, whereas the benzene-related bands should not have been affected. As can be seen in Figure 7, in the FTIR spectrum of *N*-deuterated MM the band at 825 cm^{-1} was completely absent, whereas the 780 cm^{-1} event remained mostly unchanged. Taking into account this finding, as well as known vibrational properties of imidazole and benzene derivatives,[23,24] we assigned the modes at 780 and 825 cm^{-1} to the in-phase C—C—C bending (ν_6) of benzene and out-of-plane deformation of imidazole rings, respectively.

Alkyd resin—medetomidine systems

It should be stressed that the spectral transformations observed in the AR–MM films were quite similar for both types of alkyd resins. Therefore, we have assumed that all findings and conclusions for one type of AR also are true for the other type, unless a difference between them was clearly observed. Solid-state infrared spectra of pure alkyd resin and medetomidine are depicted in Figure 8, from which it can be seen that the peaks of both compounds strongly overlapped. Only a few spectral bands (marked with arrows) could reasonably be used as internal standards for comparison of spectral variation. In the spectra of the AR–MM mixtures (data not shown), the most prominent transformation occurring with increasing medetomidine content was the continuous growth of the characteristic MM peaks in the region of 750–1600 cm^{-1} and of a wide structureless band between 2400 and 3400 cm^{-1}. In addition, the shapes and positions of many peaks characteristic of both compounds showed clear dependence on the C_p/C_m ratio. These changes are discussed in more detail below.

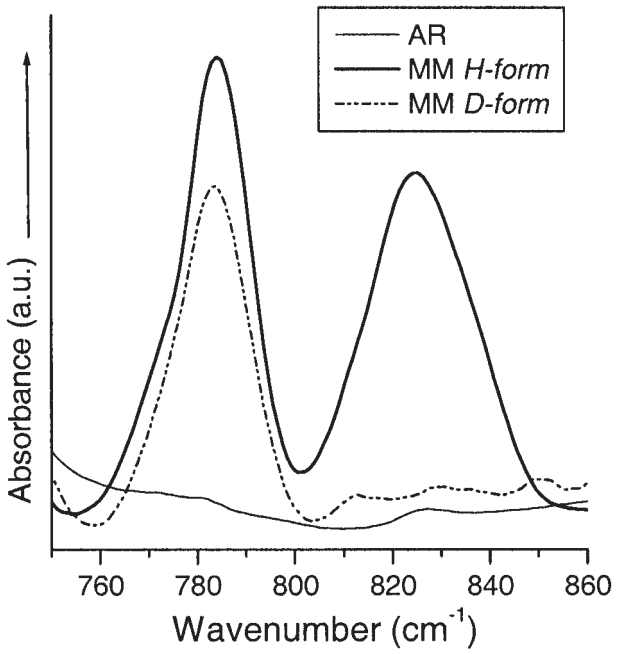

Figure 7 Comparison of FTIR spectra of medetomidine in protonated and deuterated forms in the frequency range of interest (see text for details).

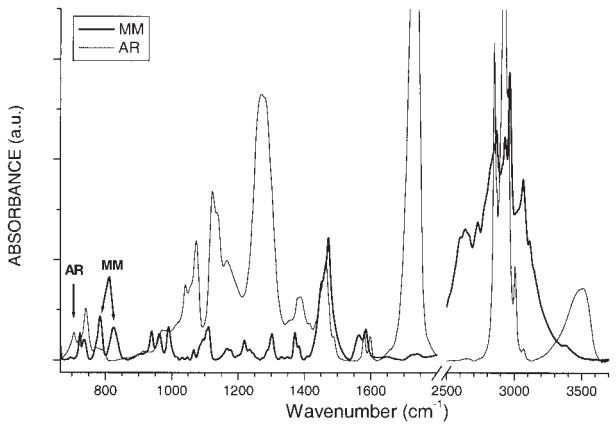

Figure 8 Comparison of infrared spectra of alkyd resin (ST-23) and medetomidine (arrow marks nonoverlapped bands).

Medetomidine bands

Figure 9 compares the spectra of alkyd-medetomidine systems of different composition in the spectral range of characteristic MM bands (see Fig. 7 and related discussion). We note here that for lowest MM contents studied in this work (C_p/C_m = 60 and 40), the intensity of the bands was too low for detailed analysis. For ST-11 resin [(Fig. 9(a)], both MM peaks showed continuous intensity increases, whereas the shape of the bands remained mainly unchanged. In contrast, in ST-23-based mixtures [Fig. 9(b)], it was noted that at low levels of added MM (large C_p/C_m ratio), the original shape of the discussed bands (shown in Fig. 7) was significantly distorted. The mode at 780 cm^{-1}, assigned to the benzene ring, demonstrated an intensity redistribution between the components, whereas their frequency position remained unchanged. For the

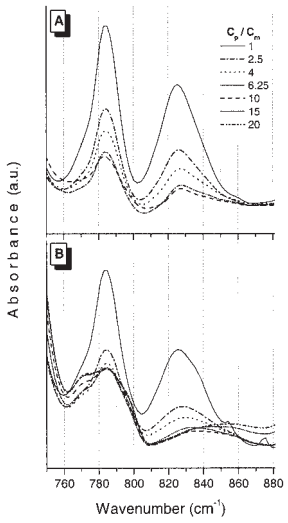

Figure 9 Comparison of FTIR spectra of different AR–MM systems in the frequency range of characteristic medetomidine vibrations: (a) ST-11, (b) ST-23.

imidazole band (825 cm^{-1}), in contrast, the intensity redistribution was not so obvious, but both components showed a shift toward higher wave numbers. A close look at the behavior of the discussed bands allowed for the assumption that starting from a certain composition, the coordination between AR and MM changed its character. This observation was in good agreement with the structural data and the NMR results. Analysis of the spectral profiles showed that essential changes in MM diffusion occurred at a C_p/C_m concentration of 6.

Carbonyl and hydroxyl bands of AR

The addition of medetomidine to the alkyd resin also caused several specific transformations in the spectral bands of the latter. First, we were interested in the behavior of characteristic bands of carboxyl groups, —COOH, (around 1710 and 3450 cm^{-1}), because these groups were those most expected to interact with the antifouling agent. It is well known that a carboxylic group is highly acidic and easily releases a proton in the presence of a hydrogen acceptor. Dissociation of carboxyl group results in formation of a carboxylate anion (—COO^-). In this anion the electrons were delocalized significantly, and the negative charge was dispersed on both oxygen atoms because of resonance. Accordingly, infrared absorption bands from C═O and OH stretching vibrations disappeared from the spectrum. Instead, the new bands arose around 1400 and 1520 cm^{-1}, characteristic of symmetric and asymmetric vibrations, respectively, rise, of —COO^- ions.[25,26] Therefore, in the systems under investigation it was expected that there would be decreased intensity of C═O and OH bands of AR with an increase in MM content. This specific behavior was observed previously[15] in mixtures of MM with another type of alkyd resin.

The spectral profiles of the characteristic band of C═O stretching vibration in pure ST-23 resin and its mixtures with medetomidine are shown in Figure 10. It can be seen that changes in film composition caused variation in all three parameters of the spectral band (frequency position, intensity, and width). The most prominent change was observed in intensity, which is discussed in detail below. In addition, as the amount of medetomidine increased, the C═O band demonstrated a progressive shift toward higher frequencies accompanied by band narrowing (Fig. 10). At the highest MM content investigated in this work (C_p/C_m = 1), in both systems we observed a shift of 6 cm^{-1} and a decrease of bandwidth of 4 cm^{-1}. The observed behavior clearly suggested the presence of a strong interaction between a polymer and an antifouling agent.

To perform a numerical analysis of the variation in carbonyl band intensity, it was important to normalize the spectra of all samples properly. The details of this normalization procedure are given in the section of the appendix on curve fitting. Figure 11 shows the calculated values of C═O band intensity for different AR–MM systems. All values were normalized with that of pure AR, such that this value equaled 1. In both systems considered in this work we noted that even at the lowest MM content, the integral intensity of the carbonyl band decreased drastically to about 30% of

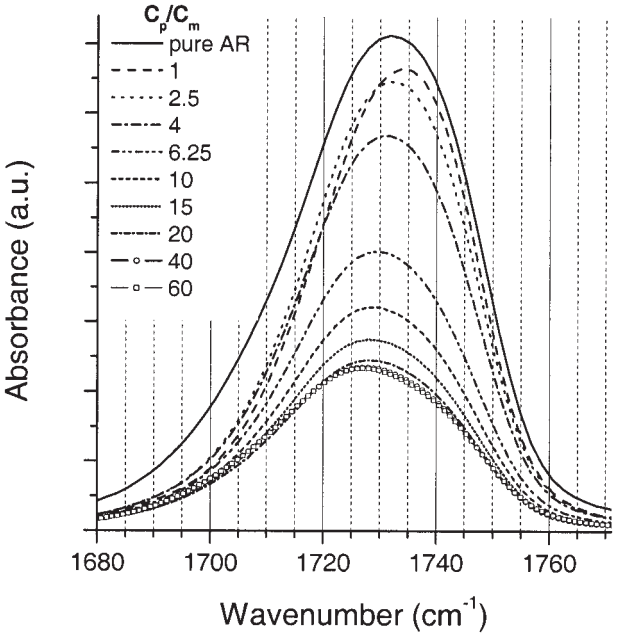

Figure 10 Variation of carbonyl band profile in AR–MM mixtures as a function of composition (ST-23). Spectra were normalized with the intensity of the AR band at 700 cm^{-1}.

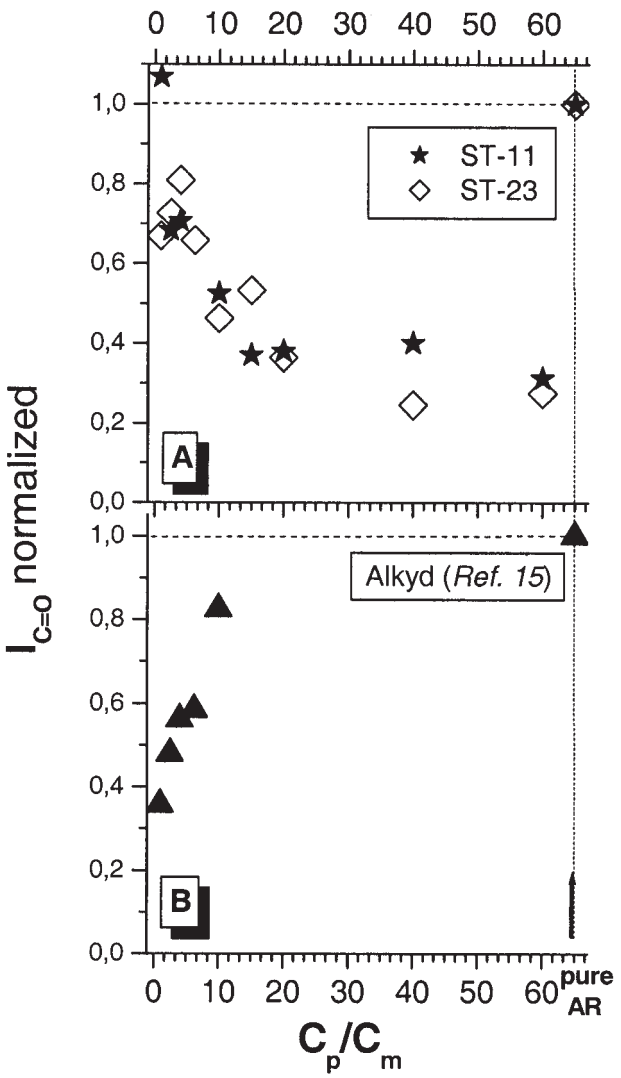

Figure 11 Total integral intensity of C═O band in different AR–MM films as a function of composition: (a) systems investigated in present study, (b) systems investigated by Shtykova et al.[15]

its initial value. This phenomenon can be explained by extensive dissociation of COOH groups. It should be noted that the extent of dissociation was very high because the remaining 30% of the intensity must be attributed to the noncarboxylic C═O groups [see Fig. 1(b)]. A complete dissociation of carboxyl groups at the lowest MM concentration was somewhat puzzling because the relative low amount of MM. Simple calculations showed that at $C_p/C_m = 60$, the NH/COOH ratios (α) were about 0.2 and 0.42 for ST-23- and ST-11-based mixtures, respectively (Table I). Therefore, it was reasonable to assume that one molecule of medetomidine interacted with several carboxyl groups of AR.

The low intensity of the C═O band remained practically constant within a wide range of MM concentrations up to $C_p/C_m = 15$ (Fig. 11). With additional increases in medetomidine content, the intensity of the C═O band started to grow, such that at the highest C_p/C_m value, it reached the magnitude observed for pure polymer. This increase can only be explained by the transformation of carboxylate anions into carbonyl groups because of either localization of the proton at one of the oxygen atoms (association of —COOH) or chemical bonding between $—COO^-$ and another species (formation of —COOR).

The behavior demonstrated by the present systems was completely different from that observed in our earlier work,[15] in which another type of AR was used as a binder. Figure 11(b) shows the variation in intensity of the CO band the systems in our previous study.[15] It can be clearly seen that spectral changes corresponded more to the expected scenario, that is, the more MM was added, the greater was the dissociation of the carbonyl groups observed. Possible reasons for such discrepancies are analyzed later in this article.

Additional evidence of the interaction between a polymer matrix and an antifouling agent was obtained from observation of the characteristic bands of OH stretching vibrations. Typically, an alkyd resin contains two types of hydroxyl groups [Fig. 1(b)], with quite different properties. Unlike acetic OH groups (—COOH), alcohol-type hydroxyl groups ($—CH_nOH$) have very low acidity and usually do not dissociate. Thus, when a hydrogen bond acceptor (like MM) is added to the AR, the expected transformation of the OH profile [Fig. 6(c)] is a decrease in total intensity because of dissociation of the carboxylic OH and possibly a redistribution of intensity because of the involvement of alcoholic hydroxyls in hydrogen bond formation.

Figure 12 compares the OH stretching profiles of pure alkyd resin and different AR–MM mixtures. In a manner similar to the C═O band, the addition of a small amount of MM caused a drastic decrease in OH band intensity. It can be seen in Figure 12 that at $C_p/C_m = 60$, integral intensity in the spectral region of 3200–3600 cm^{-1} was essentially lower than that of pure AR. Despite that, several spectral components could still be resolved. Such behavior agreed well with the decreased C═O intensity and may be explained by dissociation of the carboxylic OH groups. The remaining peaks in this region could be ascribed to alcohol-type OH groups, which did not dissociate in the presence of medetomidine. With the further addition of MM, the main change in this spectral region was growth of a wide high-frequency "wing." This is a characteristic feature of medetomidine (see Fig. 8), and its rise was obviously determined by the increasing MM content.

Unfortunately, a comprehensive curve fitting procedure in the OH characteristic region was impossible because of the strong overlap of the spectral bands.

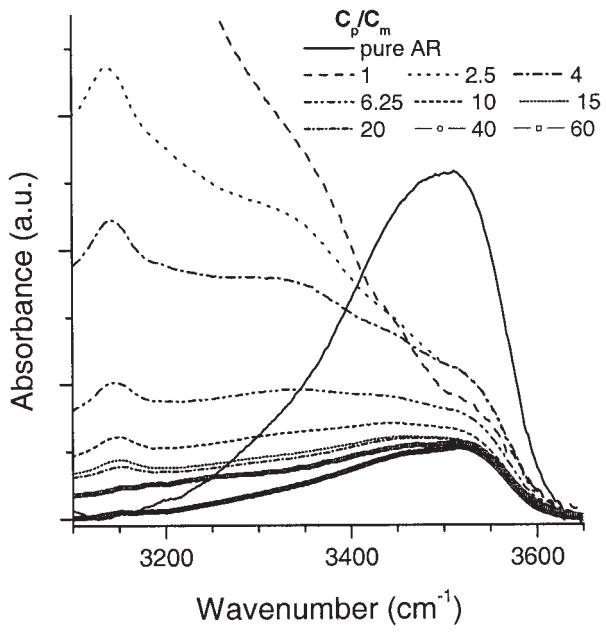

Figure 12 Evolution of the OH stretching vibrations band in the AR–MM mixture (ST-23) as a function of composition.

Nevertheless, from visual analysis we were able to conclude that the intensity of the OH bands very weakly varied with medetomidine content or did not change at all. Therefore, it could reasonably be concluded that formation of OH groups did not occur at any level of MM addition.

Mechanisms of AR–MM coordination/interaction

On the basis of experimental NMR and FTIR findings and observations, we have tried to construct a dynamic picture of medetomidine–alkyd resin interactions.

The FTIR data unambiguously showed that the carboxyl groups in the ST-11 and ST-23 alkyd resins dissociated completely even at very low levels of added antifoulant. Spectral signals corresponding to both parts of these species—carbonyl at about 1725 cm^{-1} and hydroxyl around 3400 cm^{-1}—vanished. With a further increase in MM content, an association of carboxylic groups occurred but without formation of the corresponding OH groups. This spectral behavior clearly suggests a chemical reaction between the two compounds, most likely an ionic association of carboxylic groups with MM molecules. This type of AR–MM interaction is not straightforward, however, and requires further clarification. Several questions must be answered: (1) Is such reaction possible in principle? (2) If yes, what reaction products would be expected? (3) How would these chemical transformations affect the NMR and FTIR spectra?

Considering the first two questions, it should be noted that although the benzene ring showed rather high stability, it is possible for the imidazole ring to participate in nucleophilic reactions.[27,28] Moreover, it was found[28] that if an electron-withdrawing group is directly linked to an imidazole, the nucleophilic addition may occur in positions 4 and/or 5 of the ring even under mild conditions (i.e., without quaternization; Scheme 1). Because a carboxylate anion may easily withdraw an electron, its reaction with the imidazole ring is probable under ambient conditions. Support for this scenario was directly obtained from the ^{1}H-NMR spectra (Fig. 3), in which distortion of olefinic 5–position protons of the imidazole ring (at 6.6 ppm) could be clearly observed.

The influence of such pronounced structural changes of MM on its vibrational spectrum is not clear, however. In our FTIR experiments the largest changes were the broadening and downward shift of the imidazole-related spectral bands with a low content of medetomidine. No other significant changes, that is, the appearance of new peaks or the vanishing of already existing ones, were noted (see Fig. 9 and corresponding discussion). To further investigate the effect of the suggested imidazole ring modification on the IR spectrum, we performed theoretical calculations of vibrational properties of MM molecules [Fig. 1(a)] and its derivative containing a bromide-substituted MM molecule at position 5 of the imidazole ring (see the Theoretical calculations section of the appendix). They apparently were quite similar. In the frequency region of interest (700–850 cm^{-1}), the main alteration was a high-frequency shift of the spectral bands of the bromide-substituted MM molecule compared to those of the MM. As discussed above, this type of change, that is, the shift of imidazole modes toward higher wave numbers, was observed in the experimental spectra (see Fig. 7 and corresponding discussion).

Summarizing all the findings of this study, we were able to determine the mechanism of interaction between medetomidine and ST-type alkyd resins, a description of which follows. Small amounts of MM caused extensive dissociation of the carboxylic groups of the alkyd resin, clearly suggesting coordination of one MM molecule with several —COOH species. As a result, carboxylate anions ($—COO^-$) were formed. Such behavior was observed for MM concentrations of $\alpha < 1$. As the number of MM molecules increased to equal or be larger than the number of carboxyl groups ($\alpha \geq 1$), formation of —COOR complexes began. This was most probably a result of the reaction between $—COO^-$ and the MM imidazole rings (nucleophilic addition), leading to ionic association between two compounds. At very high MM contents ($\alpha > 5$), the signs of free, that is, nonbonded, MM molecules could be clearly

observed. It was seen as a rapid increase in the MM self-diffusion coefficient in solution (see Fig. 5) and as the presence in the films of peaks characteristic of a pure solid compound (spectra not shown).

It is important to note that the MM–AR coordination was significantly different from that observed previously[15] for another type of AR [compare Fig. 11(a,b)]. However, the relative number of carboxylic groups in that material (acidity of the resin) was practically the same as that in ST-11 (10.5 vs. 11.5), but the chain length and structural organization were different. Thus, it is reasonable to suggest that the strength and mechanism of the MM–AR interaction depended not only on the acidity of AR but also on the structure of the chains to which these groups were attached. To verify this premise, we investigated mixtures of MM with two carboxylic acids (see the Spectra of model solutions section of the appendix); the results clearly showed that such dependence really exists.

CONCLUSIONS

The intermolecular interactions between medetomidine, a novel antifouling agent, with two types of middle-oil alkyd resins used as polymer binders in industrial marine paints were investigated by NMR and FTIR techniques. The strength and mechanisms of MM–AR coordination was studied in liquid solution and solid film as a function of polymer-to-antifoulant ratio. When present at low content, MM coordinated with alkyd resin mostly through hydrogen bonding of carboxyl groups of resin with imidazole rings of antifoulant. This interaction had a multidentate character (i.e., one molecule of MM interacted with several —COOH species of AR), resulting in stronger bonding between the two compounds. Starting from a certain ratio of MM and carboxyl groups to AR, estimated to be about 1 : 1, the ionic association between them began. With further increases of MM content, microphase separation occurred: excess antifoulant crystallized out of the film.

It should be stressed that the strong interaction between medetomidine and the alkyd resins investigated may be a very positive factor from the application point of view. In fact, for usual marine paints it is desirable to have quite weak polymer–antifoulant bonding in order to provide good release of the latter into water. The situation is different, however, with self-polishing paints. There the interaction must be very strong in the absence of water but should be much weaker once water is allowed to penetrate the paint. Therefore, we have concluded that the use of medetomidine as an antifouling agent and of alkyd resin (or similar molecules) as a binder may work very well for self-polishing marine paints.

It also should be noted that despite good correlation between the behavior of the components in model solutions with that in real paint coatings, the effect of other paint components cannot be eliminated completely.

The authors thank the Swedish NMR center for granting spectrometer time. Dr. P. Johansson is greatly acknowledged for his help with the theoretical simulations.

APPENDIX

Curve fitting

Deconvolution of complex spectral profiles was performed using SpectraCalc, commercial software from Jandel Scientific Ltd. The analysis of all spectra was carried out under identical conditions and in the same spectral regions: 670–760 and 1675–1775 cm^{-1}. Typical results of the curve-fitting procedure are shown in Figure A1. In the low-wave-number region, consisting of a series of strongly overlapped bands [Fig. A1(a)], we used five spectral components, the minimum number that would provide a satisfactory fit. In the carbonyl region [Fig. A.1(b)], we used three components, as discussed above.

To get optimal results, all three parameters (frequency, intensity, and width) were released for all peaks. In the 670–760 region, however, special care was taken to assure that the fit results were similar for all spectra. Then the integral intensity of the spectral band at 705 cm^{-1} [shaded in Fig. A1(a)] was used as a normalization factor. The intensity of the band of carbonyl stretching vibration was determined as a sum of integral intensities of all three spectral components [Fig. A.1(b)]. Thus, the normalized intensity of C═O vibrations depicted in Figure 11 was calculated as a ratio, $I_{TOTAL}(1675–1775)/I(705)$.

Theoretical calculations

Calculations of IR active vibrational modes were carried out with two similar molecules: medetomidine [shown in Fig. 1(a)] and the model compound depicted on the right in Figure A.2. To simulate the chemical bonding of MM via the nucleophilic addition to the 4-position of the imidazole ring, we selected the MM-like molecule in which one of the bonds is substituted with a heavy atom. Figure A.2 (left side) shows the results of theoretical calculations for two molecules along with an experimental FTIR spectrum. Two important comments should be made here. First the calculations were made for free molecules (i.e., in the gas phase), whereas experimental spectrum was taken from the solid compound. Second, the observed broadening of both bands of interest, 785 and 825 cm^{-1}, appears to have occurred because of removal of

degeneracy of the corresponding vibrations and cannot be accounted for by the present calculations. Taking into account these corrections, rather good agreement between the experimental and theoretical results can be noted. Our main interest, however, was the possible transformation of the infrared spectrum of the MM molecule at opening of one of the double bonds of the imidazole ring. Calculations showed that such structural changes will not cause essential changes in the infrared spectrum. Only an upward frequency shift of both vibrational modes for about 20–25 cm^{-1} and small intensity redistribution were expected. This prediction completely agreed with the experimental observations presented in Figure 9 and discussed in the text.

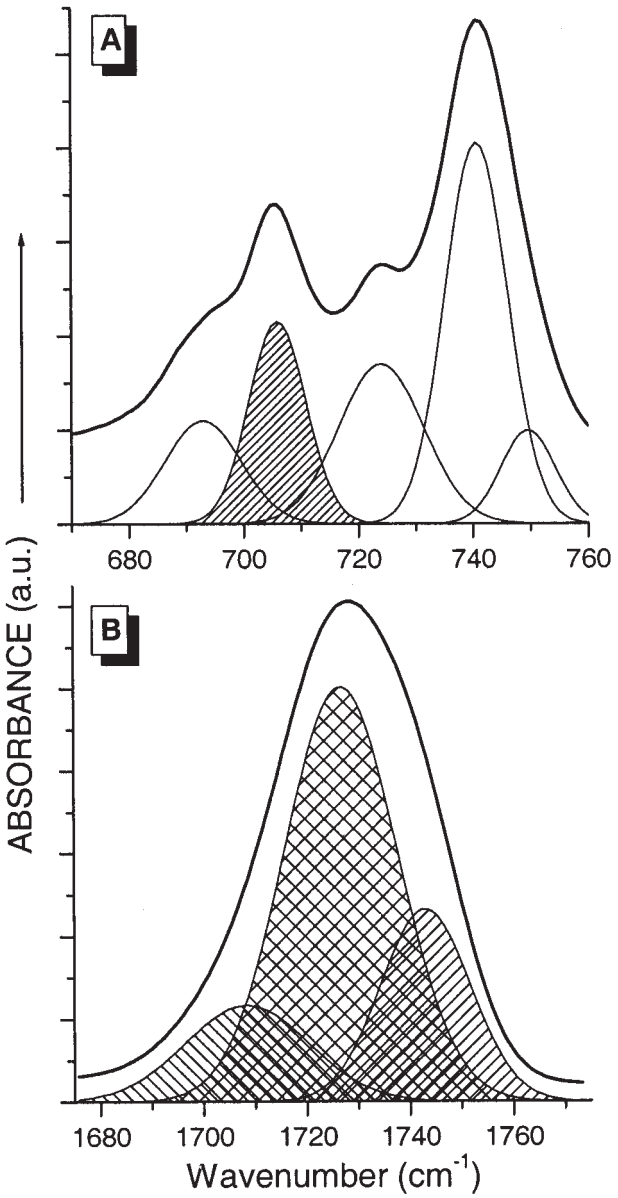

Figure A.1 Typical results of curve fitting procedure in the spectral regions of interest.

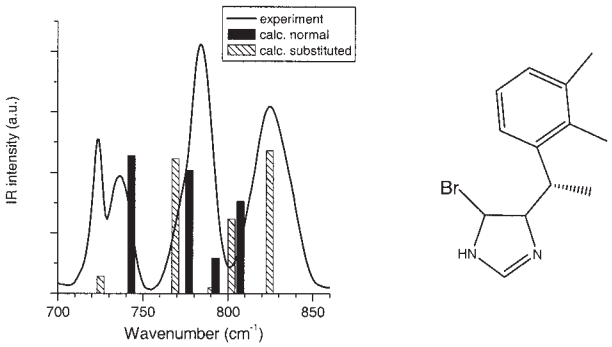

Figure A.2 Theoretically calculated vibrational modes of MM molecule [see Fig. 1(a)] and its derivative (model compound shown on right).

Spectra of model solutions

Because the observed behavior was different from that reported above, we decided to test the molecular coordination (type of bonding) between medetomidine and several compounds containing carboxyl groups. The main aim was to investigate the effect of the surrounding —COOH group on its reaction to the MM molecule. Thus, a set of model solutions was prepared by dissolving controlled amounts of MM and the model compound in xylene. The FTIR measurements were carried out in the same way as for the samples investigated in this work, that is, by drying the mixture and measuring the spectra of the remaining solid film.

Two systems were investigated.

1. *Mixture of MM with acetic acid*, AA (CH_3COOH). In this case, after evaporation of the solvent, the spectrum of the solid compound [Fig. A.3(a)] did not contain any traces of acetic acid. This can be explained by the evaporation of AA, a volatile compound, occurring together with the xylene. This means, in turn, that the interaction between MM and AA molecules was quite weak and most likely occurred via hydrogen bonding.
2. *Mixture of MM with myristic acid*, MA [$CH_3(CH_2)_{12}COOH$]. Unlike acetic acid, MA is not volatile and does not evaporate with the solvent. The spectra of solid MA–MM films [Fig. A3(b)] showed clear dependence on composition. Two important observations can be noted. First, the intensity of the C═O stretching band (around 1700 cm^{-1}) decreased continuously with the addition of MM. Such behavior is typical of progressive dissociation of COOH groups of myristic acid because of hydrogen bonding with MM molecules. It is interesting to mention that at a 1 : 1 molar ratio, not all the carboxylic groups of MA dissociated, signaling that the extent of MM–MA interaction was par-

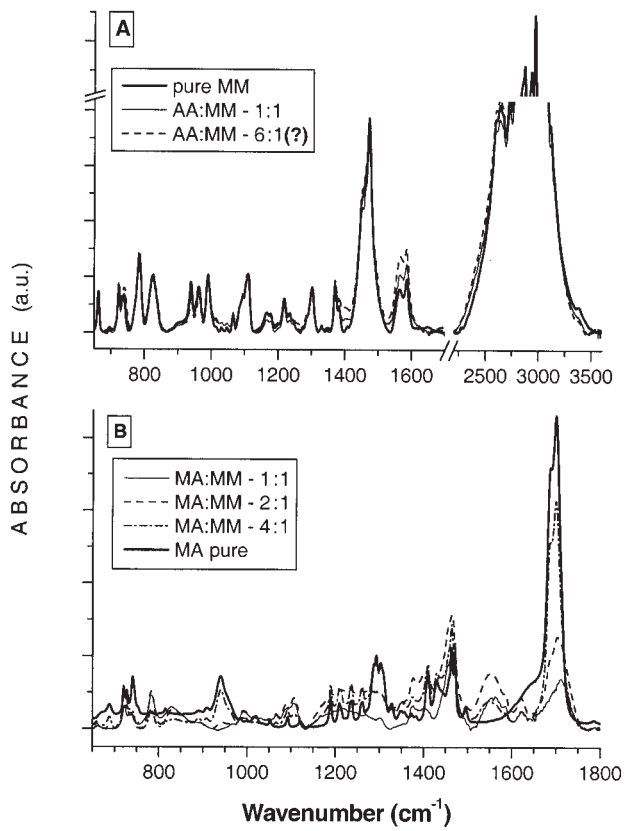

Figure A.3 FTIR spectra of model mixtures of medetomidine (MM) and different carboxylic acids: (a) acetic acid (AA) and (b) myristic acid (MA). Spectra were normalized with the intensity of the C—H stretching bands of the corresponding acid (2750–2850 cm^{-1}).

tially determined by the configuration of the chains containing carboxylic groups.

The second observation of significant importance is the obvious alteration of MA structure/conformation in the presence of MM. It can be clearly seen from Figure A.3(b) that spectral bands of the acid underwent essential changes with the addition of medetomidine. Thus, the broad intense band around 950 cm^{-1} vanished completely in MM reach mixtures. In addition, a series of sharp, well-resolved peaks in the 1150–1325 cm^{-1} region washed into a broad structureless feature in the presence of MM. This observation clearly demonstrates that medetomidine not only formed hydrogen bonds with carboxylic groups of another compound but also may have caused essential reconformation of its chains.

At the same time, no changes in the spectral profiles of MM in the region 760–860 cm^{-1} with concentration were observed. This suggests that no chemical reaction occurs between MM and MA.

References

1. International Tin Research Institute. Tin Chemicals, the Formula for Success; Publication no. 681; ITRI: Uxbridge, UK, 1987.
2. Blunden, S. L.; Cusack, P. A.; Hill, R. The Industrial Uses of Tin Chemicals. The Royal Society of Chemistry; Burlington House: London, 1985; p 41.
3. Evans, C. J.; Smith, P. J. Organotin Compounds in Modern Technology. J Organomet Chem Library, Vol. 16; Elsevier: Amsterdam, 1985; p 135.
4. Kishihara, M. Kagaku Kogyo 1998, 49, 458.
5. Omae, I. Chem Rev 2003, 103, 3431.
6. Omae, I. Appl Organomet Chem 2003, 17, 81.
7. Yamamoto, H.; Satuito, C. G.; Yamazaki, M.; Natoyama, K.; Tachibana, A.; Fusetani, N. Biofouling 1998, 13, 69.
8. Rittschof, D.; Parker, K. K. Recent Adv Mar Biotechnol 2001, 6, 239.
9. Virtanen, R.; Savola, J. M.; Saano, V.; Nyman, L. J Pharmacol 1989, 150, 9.
10. Savola, J. M.; Virtanen, R. E. Eur J Pharmacol 1991, 195, 193.
11. Maze, M.; Virtanen, R.; Daunt, D.; Banks, S. J.; Stover, E. P.; Feldman, D. Anesth Analg 1991, 73, 204.
12. Dahlström, M.; Jonsson, P. R.; Lausmaa, J.; Arnebrant, T.; Sjögren, M.; Holmberg, K.; Mårtensson, L. G. M.; Elwing, H. Biotechnol Bioeng 2004, 86, 1.
13. Dahlström, M.; Mårtensson, L. G. E.; Jonsson, P. R.; Arnebrant, T.; Elving, H. Biofouling 2000, 16, 191.
14. Surface Coatings. Vol. 2, Paints and Their Applications; prepared by Oil and Colour Chemists' Association, Australia; Chapman and Hall: London, 1984.
15. Shtykova, L. S.; Ostrovskii, D.; Handa, P.; Holmberg, K.; Nydén, M. Prog Org Coat 2004, 51, 125.
16. Holmberg, K. In Coatings Technology Handbook; Marcel Dekker: New York, 1991; p 784.
17. Stilbs, P. Prog Nucl Magn Reson Spectrosc 1987, 19, 1.
18. Stilbs, P.; Paulsen, K.; Griffiths, P. C. J Phys Chem 1996, 100, 8180.
19. Reichardt, C. Solvents and Solvent Effects in Organic Chemistry, 3d ed.; Wiley-VCH: Weinheim, Germany, 2003; 629 p.
20. Socrates, G. Infrared Characteristic Group Frequencies; Wiley: New York, 1994.
21. Zundel, G. Hydration and Molecular Interaction; Academic Press: London, 1969.
22. Hodgson, J. B.; Percy G. C.; Thorton, D. A. J Mol Struct 1980, 66, 75.
23. Varsanyi G.; Szoke, S. Vibrational Spectra of Benzene Derivatives; Academic Press: New York and London, 1969.
24. Bellocq, A.-M.; Garrigou-Lagrange, C. J Chim Phys Physico-Chim Biol 1969, 66, 1511.
25. Redington, R. L.; Lin, K. C. Spectrochim Acta Part A 1971, 27A, 2445.
26. Petrick, R. A.; Wilson, A. D. Spectrochim Acta Part A 19741, 30A, 1073.
27. Itoh, T.; Hasegawa, H.; Nagata, K.; Ohsawa, A. J Org Chem 1994, 59, 1319.
28. Ohta, S.; Osaki, T.; Nishio, S.; Furusawa, A.; Yamashita, M.; Kawasaki, I. Tetrahedron Lett 2000, 41, 7503.